

Supporting Information

Synthesis and Magnetic Properties of 2,2-Diphenyl-1,2-dihydroquinoline *N*-Oxyl Carrying Ethynyl Group at 5-Position

Masaomi Takii, Fumiteru Nishiura, Masaru Yao, Hidenari Inoue, Youhei Miura, and Naoki Yoshioka*

Department of Applied Chemistry, Faculty of Science and Technology, Keio University, Yokohama 223-8522, Japan

E-mail: yoshioka@applc.keio.ac.jp

Table of contents

General methods	2
Experimental details	3
EPR simulation parameters	6
UV-vis measurement	7
Cyclic voltammetry	8
Crystallographic parameter	9
IR spectra	10
Orbital energy level	11
Distribution of spin density	13
Magnetic interaction	16
¹ H and ¹³ C NMR charts	19
References	24

General methods

All commercially available chemical compounds were used without further purification unless otherwise noted. The ^1H and ^{13}C NMR spectra were recorded on a JNM-ECA500 (500 MHz), JEOL JNM-ECS-400 (400 MHz), or JEOL JNM-ECZ-400 (400 MHz) NMR spectrometer, and the chemical shifts are given in parts per million (ppm) relative to tetramethylsilane ($\delta = 0.00$ ppm). The elemental analyses were carried out at the Central Laboratory of the Faculty of Science and Technology, Keio University. The X-ray diffraction data were collected by a Bruker D8 VENTURE diffractometer with Mo $K\alpha$ (0.71073 Å) and Cu $K\alpha$ (1.54178 Å) radiation. The structures were solved by the intrinsic phasing method, and the non-hydrogen atoms were anisotropically refined with full matrix least-squares using SHELXL-2019/1^{S1} in the Bruker APEX4 v2021.10-0 program package.^{S2} Hydrogen atoms were placed in calculated positions and refined using a riding model. Mass spectrometry was performed using a Bruker tims-TOF Pro 2 (high-resolution, ESI) instrument. IR spectra were recorded using a Bruker ALPHA system. All IR measurements were performed by the attenuated total reflectance (ATR) method. Strong, medium and weak signals are represented by (s), (m) and (w) in experimental details section, respectively. The magnetic susceptibility measurements were carried out using Quantum Design MPMS-XL7 EC and MPMS-5 EC SQUID magnetometers. The diamagnetic contribution from the sample holder and samples were estimated and corrected using the Pacault method.^{S3} The X-band EPR spectra were recorded using a Bruker E500 spectrometer. The signal centers were calibrated by a Bruker ER035M Tesla meter. The samples were degassed by the freeze–pump–thaw method. UV-vis absorption spectra of solutions were measured using a JASCO V-650 instrument. All the theoretical calculations were conducted using a suite of Gaussian 16, Revision C.01 program.^{S4}

Experimental details

5-Aminoquinoline^{S5}

5-Nitroquinoline (6.10 g, 34.7 mmol, 1 eq.) and $\text{SnCl}_2 \cdot 2\text{H}_2\text{O}$ (39.1 g, 173.5 mmol, 5 eq.) were dissolved in EtOH (150 mL), and the mixture was stirred for 30 min at reflux temperature. After cooling to room temperature, the reaction mixture was neutralized with saturated aqueous NaHCO_3 and extracted with EtOAc. The combined organic layers were dried over Na_2SO_4 and concentrated under reduced pressure. The residue was purified by column chromatography (EtOAc) to afford the title compound as a pale yellow solid (4.983 g, quant.). Mp 108-111 °C ; $^1\text{H-NMR}(\text{CDCl}_3, 400 \text{ MHz})$: δ = 8.90(dd, 1H, J = 4.0, 2.4 Hz), 8.19(dd, 1H, J = 8.0, 0.8 Hz), 7.59-7.50(m, 2H), 7.36(dd, 1H, J = 8.0, 4.0 Hz), 6.83(dd, 1H, J = 7.2, 0.8 Hz), 4.20(s, 2H) ppm ; $^{13}\text{C-NMR}(\text{CDCl}_3, 100 \text{ MHz})$: δ = 150.4, 149.3, 142.4, 130.1, 129.6, 120.3, 119.7, 118.8, 110.1, ppm ; FT-IR : 3324(m), 3183(m), 1655(m), 1612(m), 1584(m), 1566(m), 1506(m), 1461(m), 1409(m), 1364(m), 1324(m), 1278(m), 1204(m), 788(s) cm^{-1} ; HRMS(ESI^+ -TOF) : m/z $[\text{M}+\text{H}]^+$ calcd. for $\text{C}_9\text{H}_8\text{N}_2$: 145.0760, found : 145.0768; elemental analysis calcd. (%) for $\text{C}_9\text{H}_8\text{N}_2$: C 74.98, H 5.59, N 19.43 ; found C 74.78, H 5.60, N 19.31.

5-Iodoquinoline^{S6}

5-Aminoquinoline (2.52 g, 17.5 mmol, 1 eq.) was dissolved in 37 % HCl (35 mL), and NaNO_2 (1.38 g, 19.3 mmol, 1.1 eq) was then added dropwise to the solution at 0 °C. The mixture was stirred for 30 min at 0 °C. The reaction mixture was added into KI (9.44 g, 63 mmol, 3.6 eq.) aqueous solution and allowed to stand overnight. After the reaction, the product was neutralized with saturated aqueous NaHCO_3 and Na_2SO_3 . The solid was filtered, then dissolved in 2-butanol. The combined organic layers were washed with brine, dried over Na_2SO_4 and concentrated under reduced pressure. The residue was purified by column chromatography (chloroform) to afford the title compound as a pale yellow solid (2.28 g, 51 %). Mp 105-107 °C : $^1\text{H-NMR}(\text{CDCl}_3, 400 \text{ MHz})$: δ = 8.89(dd, 1H, J = 8.4, 2.0 Hz), 8.38(d, 1H, J = 9.2 Hz), 8.11(m, 2H), 7.54(t, 1H, J = 8.0 Hz), 7.49-7.41(m, 1H) ppm ; $^{13}\text{C-NMR}(\text{CDCl}_3, 100 \text{ MHz})$: δ = 151.2, 148.7, 140.3, 137.7, 130.5, 130.4, 130.2, 122.8, 98.5 ppm ; FT-IR : 788(s) cm^{-1} ; elemental analysis calcd. (%) for $\text{C}_9\text{H}_6\text{IN}$: C 42.38, H 2.37, N 5.49 ; found C 42.28, H 2.36, N 5.46.

5-[2-(Trimethylsilyl)ethynyl]quinoline^{S7}

5-Iodoquinoline (2.33 g, 9.13 mmol, 1 eq.) was dissolved in TEA (20 mL). TMSA (1.92 mL, 13.7 mmol, 1.5 eq.), $\text{Pd}(\text{PPh}_3)_2\text{Cl}_2$ (313 mg, 0.46 mmol, 0.05 eq.), and CuI (210 mg, 1.10 mmol, 0.12 eq.) were then added, and the mixture was stirred for 16 h at 50 °C under nitrogen atmosphere. After the reaction, saturated aqueous NH_4Cl was added, and the mixture was extracted with CHCl_3 . The combined organic layers were washed with brine, dried over Na_2SO_4 and concentrated under reduced pressure. The product was purified by silica gel chromatography (EtOAc: Hexane = 1: 3) to afford the

title compound as a brown oil (1.93 g, 93 %). $^1\text{H-NMR}(\text{CDCl}_3, 400 \text{ MHz})$: δ = 8.94(dd, 1H, J = 4.4, 1.6 Hz), 8.62(d, 1H, J = 8.4 Hz), 8.09(d, 1H, J = 8.4 Hz), 7.75(dd, 1H, J = 7.2, 0.8 Hz), 7.64(m, 1H), 7.49(dd, 1H, J = 8.0, 4.0 Hz), 0.30(s, 9H) ppm ; $^{13}\text{C-NMR}(\text{CDCl}_3, 100 \text{ MHz})$: δ = 150.8, 147.8, 134.5, 131.0, 130.5, 128.7, 128.7, 121.7, 121.1, 101.6, 100.3, -0.5 ppm ; HRMS(ESI⁺-TOF) : m/z [M+H]⁺ calcd. for $\text{C}_{14}\text{H}_{15}\text{NSi}$: 226.1047, found : 226.1049; FT-IR : 2958(w), 2154(w), 1250(m), 843(s) cm^{-1} .

5-[2-(Trimethylsilyl)ethynyl]quinoline *N*-oxide^{S8}

5-[2-(Trimethylsilyl)ethynyl]quinoline (1.93 g, 8.58 mmol, 1 eq.) was dissolved in CHCl_3 (30 mL). 69 % *m*-CPBA (3.22 g, 12.87 mmol, 1.5 eq.) dissolved in CHCl_3 was added to the solution at 0 °C, and the mixture was stirred for 16 h at room temperature. The mixture was neutralized with ammonia water and extracted with CHCl_3 . The combined organic layers were washed with brine, dried over Na_2SO_4 and concentrated under reduced pressure. The product was purified by column chromatography (CHCl_3) to afford the title compound as a white solid (1.42 g, 68 %). Mp 148-150 °C ; $^1\text{H-NMR}(\text{CDCl}_3, 500 \text{ MHz})$: δ = 8.73(d, 1H, J = 8.5 Hz), 8.55(d, 1H, J = 6.5 Hz), 8.18(d, 1H, J = 8.5 Hz), 7.82(dd, 1H, J = 7.5, 1.0 Hz), 7.69(m, 1H), 7.37(m, 1H), 0.34(s, 9H) ppm ; $^{13}\text{C-NMR}(\text{CDCl}_3, 125 \text{ MHz})$: δ = 141.7, 135.9, 133.1, 131.1, 130.4, 129.6, 124.4, 122.0, 121.5, 120.4, 102.1, 100.7, -0.1 ppm ; HRMS(ESI⁺-TOF) : m/z [M+H]⁺ calcd. for $\text{C}_{14}\text{H}_{15}\text{NOSi}$: 242.0996, found : 242.0996; FT-IR : 2954(w), 2146(w), 1560(w), 1512(w), 1406(m), 1247(m) cm^{-1} ; elemental analysis calcd. (%) for $\text{C}_{14}\text{H}_{15}\text{NOSi}$: C 69.67, H 6.26, N 5.80 ; found C 69.18, H 6.26, N 5.77.

5-[2-(Trimethylsilyl)ethynyl]-2-phenylquinoline *N*-oxide^{S9}

5-[2-(Trimethylsilyl)ethynyl]quinoline *N*-oxide (1.37 g, 5.68 mmol, 1 eq.) was dissolved in dry THF (30 mL). Phenyl magnesium bromide THF solution (5.68 mL, 5.68 mmol, 1 eq.) was added, and the mixture was stirred for 1 h at room temperature under nitrogen atmosphere. An additional portion of phenyl magnesium bromide THF solution (5.68 mL, 5.68 mmol, 1 eq.) was added, and the mixture was stirred for 16 h at the reflux temperature. After cooling to the room temperature, the reaction mixture was quenched with saturated aqueous NH_4Cl and extracted with CHCl_3 . The combined organic layers were washed with brine, dried over Na_2SO_4 and concentrated under reduced pressure. The product was purified by silica gel chromatography (CHCl_3 : hexane = 1: 1) to afford the title compound as a white solid (334 mg, 19 %). Mp 148-149 °C ; $^1\text{H-NMR}(\text{CDCl}_3, 400 \text{ MHz})$: δ = 8.83(d, 1H, J = 9.2 Hz), 8.19(d, 1H, J = 9.2 Hz), 7.98(d, 2H, J = 7.2 Hz), 7.81(dd, 1H, J = 7.2, 0.8 Hz), 7.70(m, 1H), 7.60-7.49(m, 4H), 0.35(s, 9H) ppm ; $^{13}\text{C-NMR}(\text{CDCl}_3, 100 \text{ MHz})$: δ = 145.3, 142.3, 133.3, 132.7, 130.1, 129.7, 129.7, 129.6, 128.3, 123.8, 123.6, 121.7, 120.9, 101.8, 100.9, -0.1 ppm ; HRMS(ESI⁺-TOF) : m/z [M+H]⁺ calcd. for $\text{C}_{20}\text{H}_{19}\text{NOSi}$: 318.1309, found : 318.1311; FT-IR : 2955(w), 2148(w), 1248(m) cm^{-1} ; elemental analysis calcd. (%) for $\text{C}_{20}\text{H}_{19}\text{NOSi}$: C 75.67, H 6.03, N 4.41 ; found C 75.07, H 6.06, N 4.43.

5-[2-(Trimethylsilyl)ethynyl]-2,2-diphenyl-1,2-dihydroquinoline *N*-oxyl (**2**)^{S9}

5-[2-(Trimethylsilyl)ethynyl]-2-phenylquinoline *N*-oxide (230 mg, 0.724 mmol, 1 eq.) was dissolved in dry THF (3 mL). Phenyl magnesium bromide THF solution (724 μ L, 0.724 mmol, 1 eq.) was added, and the mixture was stirred for 1 h at room temperature under nitrogen atmosphere. An additional portion of phenyl magnesium bromide THF solution (724 μ L, 0.724 mmol, 1 eq.) was added, and stirring was continued for 16 h at the same condition. After the reaction, the reaction mixture was quenched with saturated aqueous NH_4Cl and extracted with CHCl_3 . The combined organic layers were washed with brine, dried over Na_2SO_4 and concentrated under reduced pressure. The product was purified by silica gel chromatography (CHCl_3 : Hexane = 1: 3) to afford dark red solid and then recrystallized from EtOH/dichloromethane to afford the title compound as a dark red crystal (84 mg, 34 %). Mp 140-141 $^\circ\text{C}$; HRMS(ESI^+ -TOF) : m/z $[\text{M}+\text{H}]^+$ calcd. for $\text{C}_{26}\text{H}_{24}\text{NOSi}$: 395.1700, found : 395.1715; FT-IR : 2961(w), 2145(w), 1246(m) cm^{-1} ; elemental analysis calcd. (%) for $\text{C}_{26}\text{H}_{24}\text{NOSi}$: C 79.15, H 6.13, N 3.55 ; found C 78.49, H 6.13, N 3.63.

5-Ethynyl-2,2-diphenyl-1,2-dihydroquinoline *N*-oxyl (**3**)^{S10}

5-[2-(Trimethylsilyl)ethynyl]-2,2-diphenyl-1,2-dihydroquinoline *N*-oxyl (540 mg, 1.37 mmol, 1 eq.) was dissolved in MeOH (50 mL). KOH aq. was added and stirred for 1 h at room temperature. The reaction mixture was quenched with saturated aqueous NH_4Cl and extracted with CHCl_3 . The combined organic layers were dried over Na_2SO_4 and concentrated under reduced pressure. The residue was purified by silica gel chromatography (CHCl_3) to afford dark red liquid. The purified liquid was recrystallized from EtOH to afford the title compound as a dark red crystal (130 mg, 30 %). Mp 131-132 $^\circ\text{C}$; HRMS(ESI^+ -TOF) : m/z $[\text{M}+\text{H}]^+$ calcd. for $\text{C}_{23}\text{H}_{16}\text{NO}$: 323.1305, found : 323.1300; FT-IR : 3225(m), 3021(w), 2102(w) cm^{-1} ; elemental analysis calcd. (%) for $\text{C}_{22}\text{H}_{18}\text{NO}_2$: C 85.69, H 5.00, N 4.34 ; found C 85.38, H 5.17, N 4.26.

EPR simulation parameters

Simulation of EPR spectra for **2** and **3** were carried out by Winsim program^{S11}.

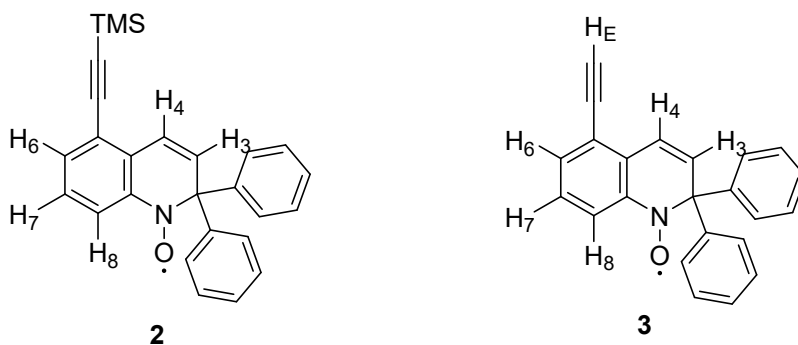


Table S1 The hfcc for nitrogen and hydrogen atoms of compound **1–3**.

	2 [G]	3 [G]	1 ^{S12} [G]
N	9.61	9.62	10.17
H ₃	1.43	1.43	1.42
H ₄	0.60	0.61	0.55
H ₆₍₈₎	3.23	3.18	3.20
H ₇	1.07	1.12	1.07
H ₈₍₆₎	3.06	3.07	3.20
H _E	—	0.42	—

UV-vis measurement

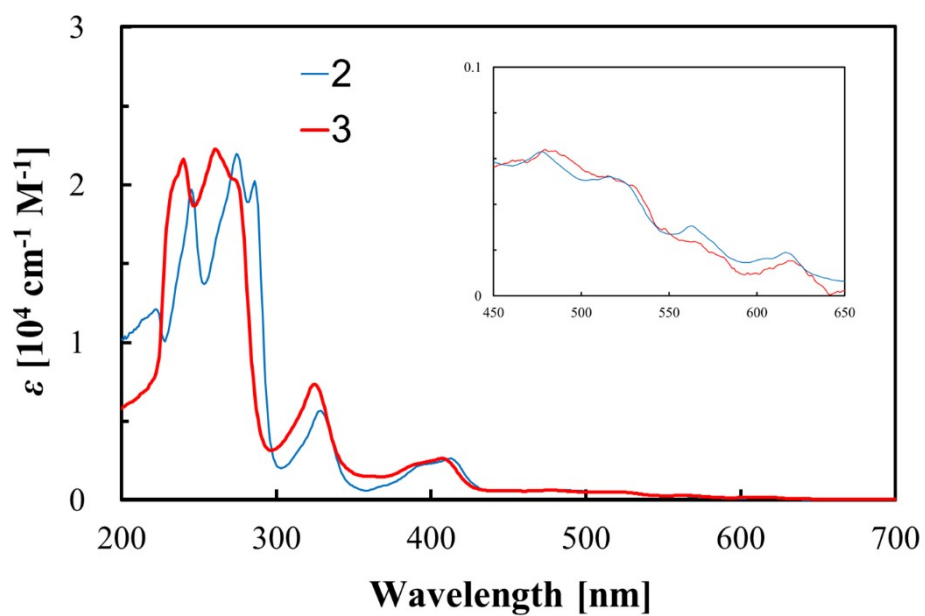


Fig. S1 UV-vis absorption spectra at room temperature of **2**(blue) and **3**(red) in 1 × 10⁻⁵ M solutions in DCM.

Cyclic voltammetry

Cyclic voltammetry measurements were carried out. The plots and redox potential were calibrated by ferrocene as internal reference. The background from the blank (only electrolyte) was subtracted to correct the data. The samples were degassed by passing nitrogen gas through the solvent. Compound **1**, **2**, and **3** showed reversible oxidation peaks at $E_{1/2} = 0.462$ V, $E_{1/2} = 0.558$ V, and $E_{1/2} = 0.569$ V, respectively.

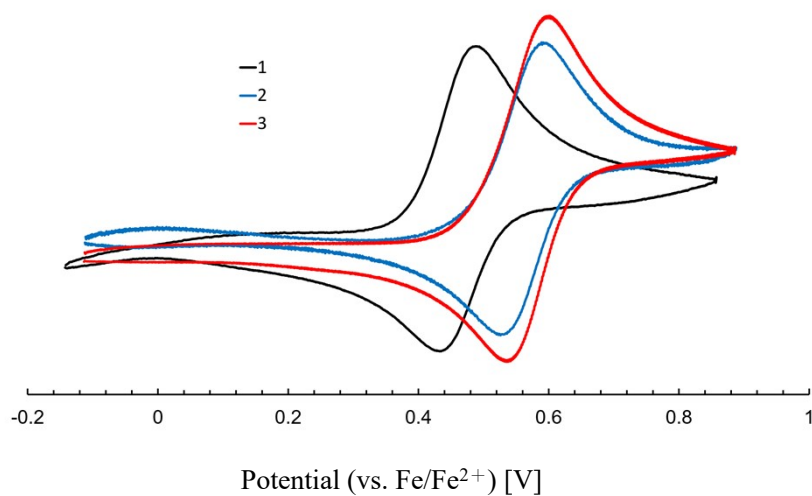


Fig. S2 Cyclic Voltammogram of **2**(blue) and **3**(red). (5.0×10^{-4} M solutions in MeCN, a GC disk electrode $d = 1.0$ mm, supporting electrolyte 0.1 M Bu₄NBF₄/MeCN, $T = 298$ K, 100 mV·s⁻¹ scan rate.)

Crystallographic parameter

	2	3	3
Formula	C ₂₆ H ₂₄ NOSi	C ₂₃ H ₁₆ NO	C ₂₃ H ₁₆ NO
<i>M</i>	394.55	322.37	322.37
Radiation type	Mo K α	Mo K α	Cu K α
Temperature [K]	90.(2)	90.(2)	90.(2)
Crystal size [mm]	0.500× 0.118× 0.072	0.720× 0.200× 0.160	0.400× 0.400× 0.200
Crystal system	monoclinic	orthorhombic	orthorhombic
Space group	<i>P</i> 2 ₁ / <i>n</i>	<i>P</i> 2 ₁ 2 ₁ 2 ₁	<i>P</i> 2 ₁ 2 ₁ 2 ₁
<i>a</i> [Å]	10.8542(3)	9.7866(5)	12.24980(10)
<i>b</i> [Å]	9.0975(2)	12.2573(7)	13.7016(2)
<i>c</i> [Å]	22.1134(6)	13.7175(7)	9.78620(10)
β [°]	93.2990(10)	90	90
<i>V</i> [Å ³]	2179.99(10)	1645.51(15)	1642.53(3)
<i>Z</i>	4	4	4
<i>D</i> [g cm ⁻³]	1.202	1.301	1.304
μ [mm ⁻¹]	0.124	0.079	0.622
<i>F</i> (000)	836	676	676
θ (min, max) [°]	2.42, 25.02	2.23, 25.03	5.56, 66.38
Index ranges	-12 ≤ <i>h</i> ≤ 12 -10 ≤ <i>k</i> ≤ 10 -26 ≤ <i>l</i> ≤ 26	-11 ≤ <i>h</i> ≤ 11 -14 ≤ <i>k</i> ≤ 14 -16 ≤ <i>l</i> ≤ 15	-14 ≤ <i>h</i> ≤ 14 -15 ≤ <i>k</i> ≤ 16 -11 ≤ <i>l</i> ≤ 8
Measured reflection	22134	17814	12516
Independent reflection (<i>R</i> _{int})	3841(0.0502)	2921(0.0491)	2873(0.0673)
Observed reflection (<i>I</i> > 2 σ (<i>I</i>))	2779	2614	2734
<i>GoF</i>	1.153	1.117	1.046
<i>R</i> , <i>R</i> _w (<i>I</i> > 2 σ (<i>I</i>))	0.0649, 0.1601	0.0433, 0.1114	0.0318, 0.0791
<i>R</i> , <i>R</i> _w (all data)	0.1025, 0.2123	0.0559, 0.1317	0.406, 0.0807
Resd density (min, max)	0.340, -0.503	0.204, -0.262	0.202, -0.181
<i>CCDC</i>	2483838	2483839	2484892

Table S2 Crystallographic parameters of **2** and **3**.

IR spectra

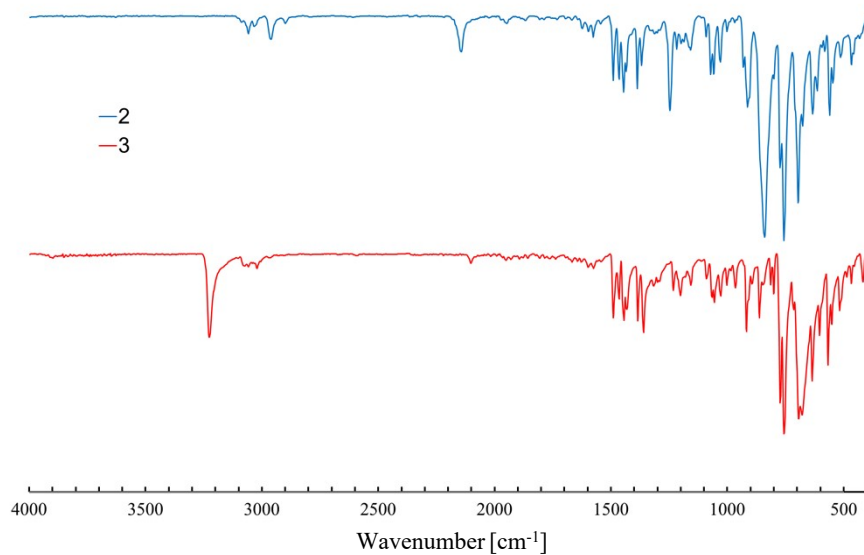


Fig. S3 IR spectra of compound **2** (blue) and **3** (red) in solid state.

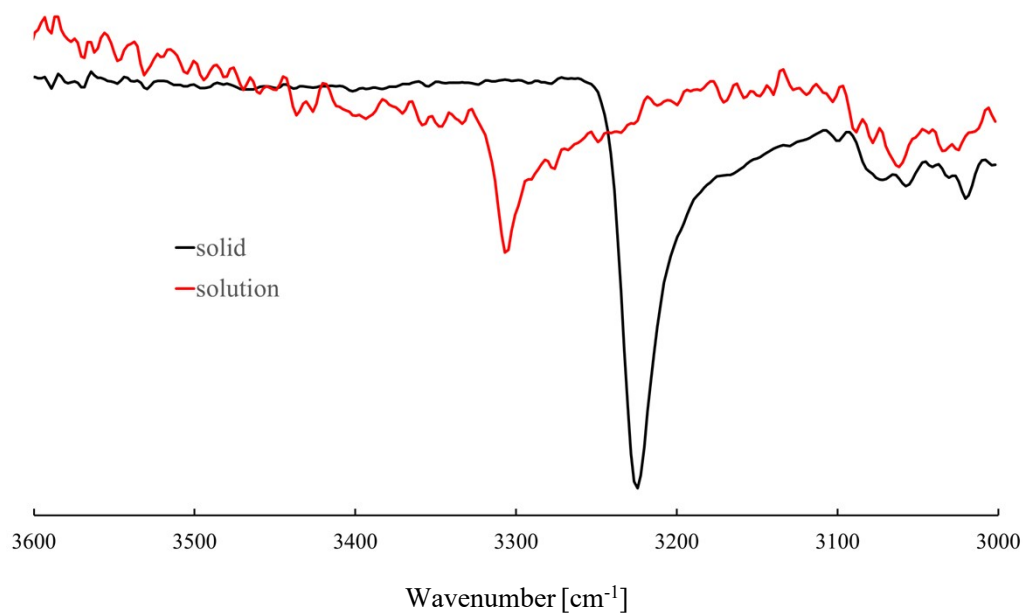


Fig. S4 IR spectra of compound **3**: solid state (black) and 5.0×10^{-4} M solution in carbon tetrachloride (red).

Orbital energy level

The calculation was performed at the UB3LYP/6-31G(d) level of theory. The coordination was obtained from crystallographic geometry.

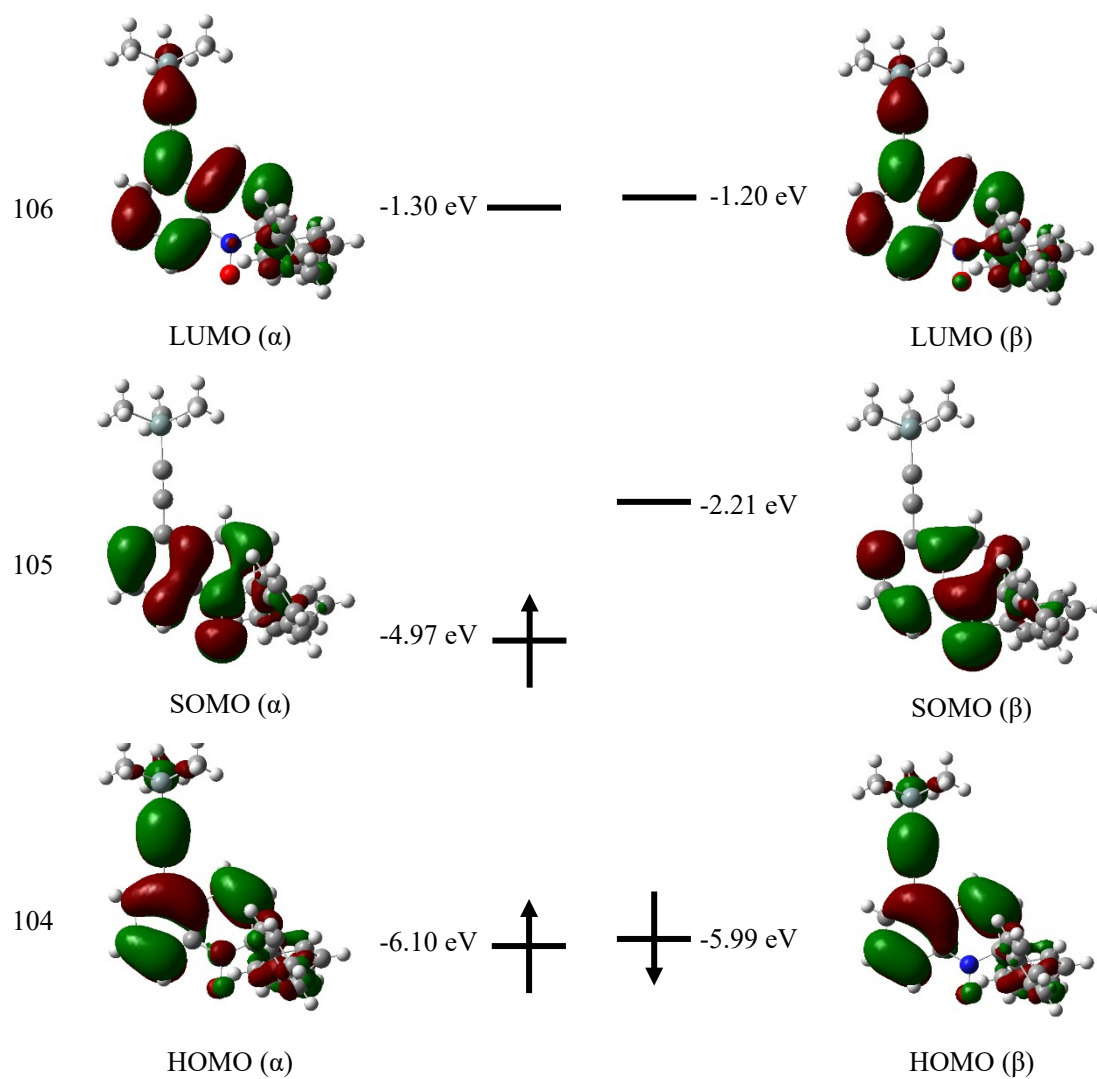


Fig. S5 Orbital energy level of **2** (UB3LYP/6-31G(d)).

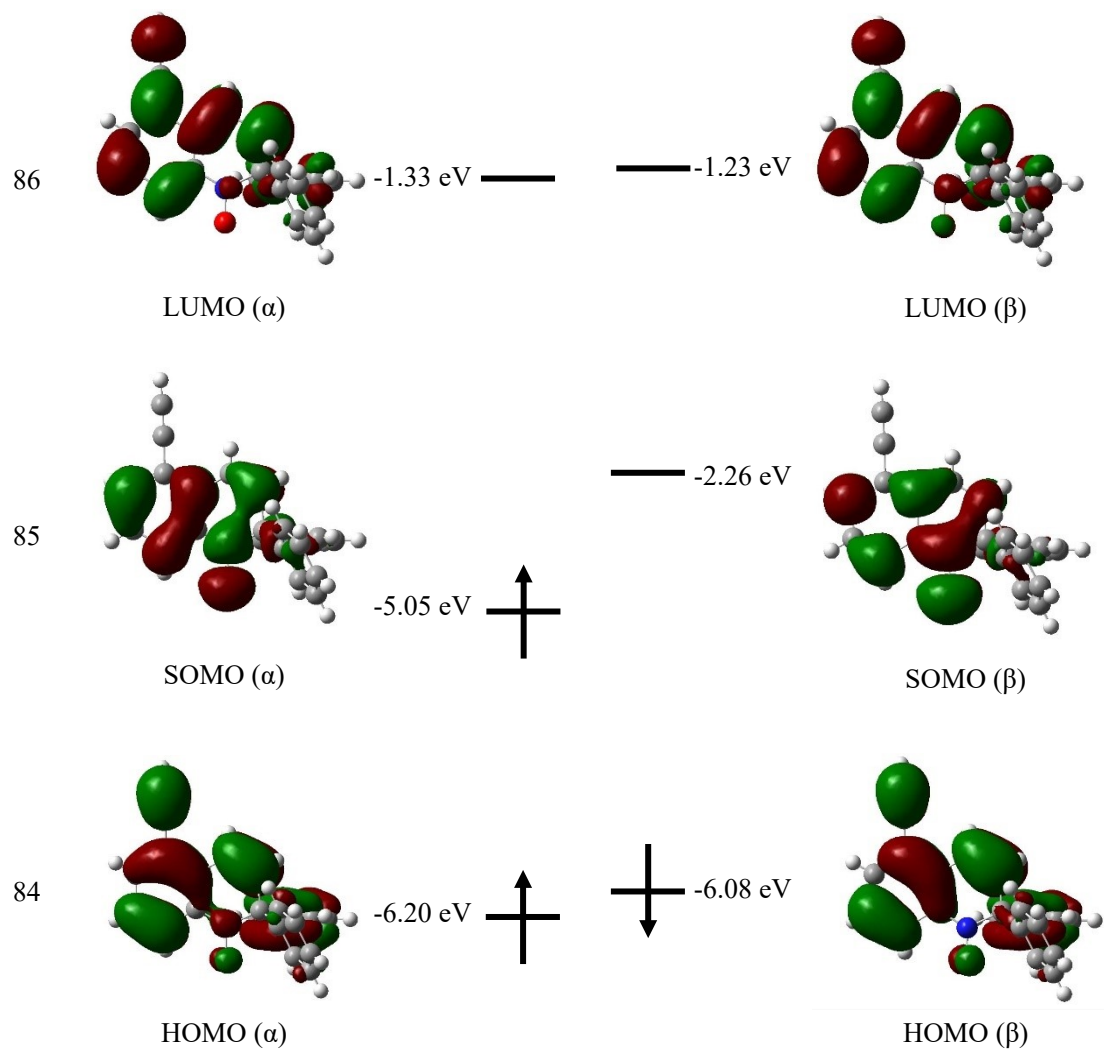


Fig. S6 Orbital energy level of **3** (UB3LYP/6-31G(d)).

Distribution of spin density

Calculated at UB3LYP/6-31G(d) level of theory.

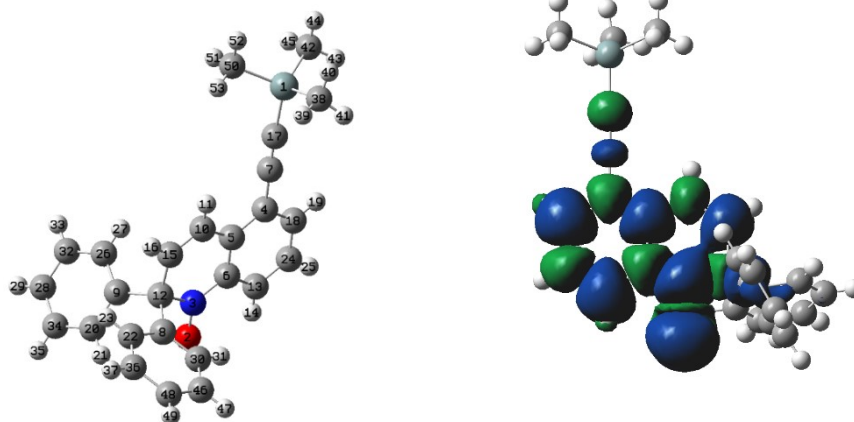


Fig. S7 Atom number (left) and spin density (right) of **2**.

Table S3 The spin density distribution on the atom of **2**.

Atom	Spin density	Atom	Spin density	Atom	Spin density
1 Si	0.000246	19 C	-0.001550	37 H	0.000140
2 O	0.482126	20 C	0.000161	38 C	-0.000778
3 N	0.338504	21 H	-0.000853	39 H	0.000036
4 C	-0.072920	22 C	0.000036	40 H	-0.000107
5 C	0.130850	23 H	-0.079715	41 H	0.000033
6 C	-0.119178	24 C	0.002753	42 C	-0.000197
7 C	0.017709	25 H	-0.001720	43 H	0.000013
8 C	0.024552	26 C	0.000324	44 C	-0.000027
9 C	0.021524	27 H	-0.001160	45 H	0.000007
10 H	-0.041447	28 C	0.000036	46 H	0.001546
11 C	0.001532	29 H	-0.002130	47 H	0.000022
12 C	-0.021910	30 C	-0.001851	48 C	-0.000009
13 C	0.153122	31 H	0.001601	49 H	-0.000028
14 H	-0.007203	32 C	0.000008	50 C	-0.000223
15 C	0.058683	33 H	0.002536	51 H	0.000008
16 H	-0.003058	34 C	0.000117	52 H	-0.000028
17 C	-0.024925	35 H	0.002156	53 H	0.000013
18 H	0.146854	36 C	-0.001550		

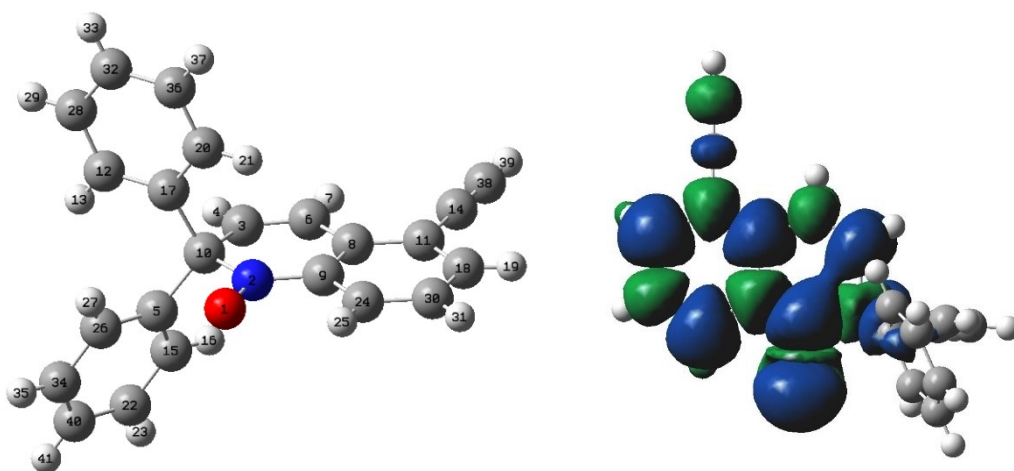


Fig. S8 Atom number (left) and spin density (right) of **3**.

Table S4 The spin density distribution on the atom of **3**.

Atom	Spin density	Atom	Spin density	Atom	Spin density
1 O	0.489493	15 C	-0.002090	29H	0.000266
2 N	0.334150	16 H	0.000705	30 C	-0.077870
3 C	0.059871	17 C	0.027537	31 H	0.002695
4 H	-0.003080	18 C	0.143528	32 C	0.000253
5 C	0.017841	19 H	-0.006080	33 H	-0.000030
6 C	-0.042570	20 C	0.000427	34 C	0.002422
7 H	0.001548	21 H	-0.001010	35 H	0.000053
8 C	0.130355	22 C	0.001894	36 C	-0.000300
9 C	-0.118310	23 H	-0.000019	37 H	0.000115
10 C	-0.021110	24 C	0.149739	38 C	-0.026410
11 C	-0.072740	25 H	-0.007060	39 H	0.000985
12 C	-0.000030	26 C	-0.002280	40 C	-0.001750
13 H	0.000060	27 H	0.000172	41 H	0.000065
14 C	0.017748	28 C	0.000791		

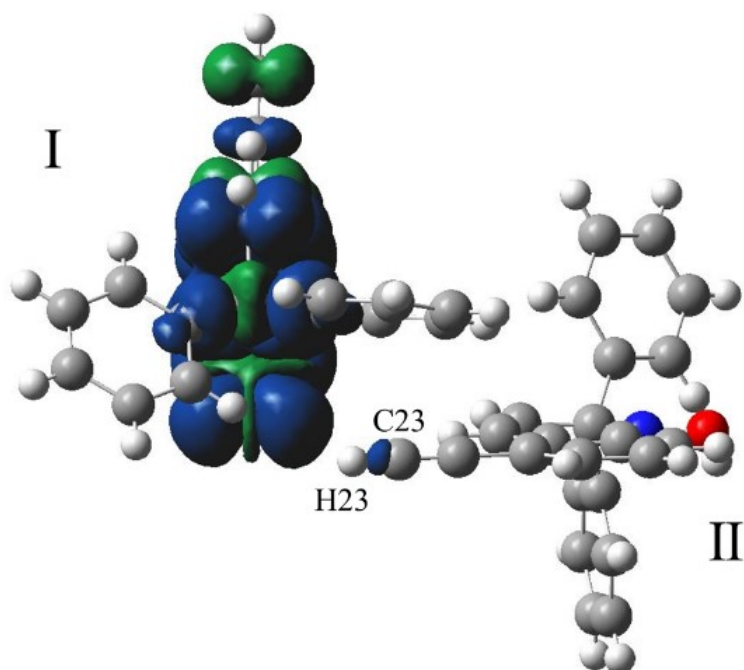


Fig. S9 Spin density distribution of ferromagnetic interacted molecules in the crystal of **3** calculated at the UB3LYP/6-31G(d) level of theory. Isovalue = 0.0004. The radical in II was inactivated by the addition of a hydrogen atom at the oxygen atom.

Magnetic interaction

The magnetic susceptibility data were fitted using Heisenberg model Hamiltonian ^{S13,14} :

$$H = -2J \sum_{\langle i, j \rangle} S_i \cdot S_j$$

Here, J represents the exchange interaction between the equally spaced neighbouring radicals i and j .

The experimental data were fitted using modified equation that takes into account the molecular field. To account for the interchain interactions, a Weiss temperature was introduced by replacing T with $T - \theta_{1D}$.

The Heisenberg 1D ferromagnetic chain model was used for fitting the data of compound **2** :

$$\chi_m = \frac{1}{T - \theta_{1D}} \frac{N_A \mu_B^2 g^2}{4k_B} \left(\frac{1 + 5.7979916 \left(\frac{x}{2}\right) + 16.902653 \left(\frac{x}{2}\right)^2 + 29.376885 \left(\frac{x}{2}\right)^3 + 29.832959 \left(\frac{x}{2}\right)^4 + 14.036918 \left(\frac{x}{2}\right)^5}{1 + 2.7979916 \left(\frac{x}{2}\right) + 7.008678 \left(\frac{x}{2}\right)^2 + 8.6538644 \left(\frac{x}{2}\right)^3 + 4.5743114 \left(\frac{x}{2}\right)^4} \right)^{\frac{2}{3}}$$

In contrast, the Heisenberg 1D antiferromagnetic chain model was used for compound **3** :

$$\chi_m = \frac{1}{T - \theta_{1D}} \frac{N_A \mu_B^2 g^2}{k_B} \frac{0.25 + 0.074975x + 0.075235x^2}{1 + 0.9931x + 0.172135x^2 + 0.757825x^3}$$

$x = |J| / k_B T$.^{S15} N_A is Avogadro's constant, μ_B is the Bohr magneton, g is the g -factor, and k_B is the Boltzmann constant.

The calculated J value ($J_{\text{calcd.}}$) was obtained from Yamaguchi's equation.^{S16}

$$J_{\text{calcd.}} = - \frac{E_{\text{BS}} - E_{\text{T}}}{\langle S^2 \rangle_{\text{T}} - \langle S^2 \rangle_{\text{BS}}}$$

The terms E is the total energy. $\langle S^2 \rangle_{\text{T}}$ and $\langle S^2 \rangle_{\text{BS}}$ represent the expectation values of the squares of the total spin operators for the T and BS solutions, respectively.^{S16}

Calculated at UB3LYP/6-31G(d) level of theory.

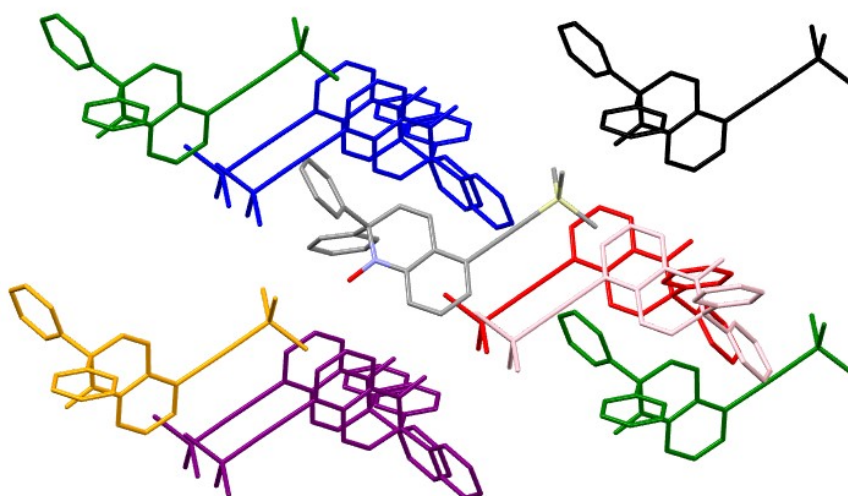


Table S5 Correspondence of name, color, and symmetry for **2**.

Contacts	Color	Symmetry
J_1	Red	$(1-x, 1-y, 1-z)$
J_2	Blue	$(1/2-x, 1/2+y, 1/2-z)$
J_3	Green	$(-1/2+x, 1/2-y, -1/2+z)$
J_4	Orange	$(1/2+x, 3/2-y, -1/2+z)$
J_5	Pink	$(1-x, 2-y, 1-z)$
J_6	Purple	$(3/2-x, -1/2+y, 1/2-z)$
J_7	Black	$(1/2+x, 1/2-y, -1/2+z)$

Table S6 Calculated J value and corresponding parameters for **2**.

Compound	$E_{BS}/\text{Hartree}$	$E_T/\text{Hartree}$	$\langle S^2 \rangle_{BS}$	$\langle S^2 \rangle_T$	$2J_{\text{calcd.}}/\text{cm}^{-1}$
2-J_1	-2848.5487789	-2848.5487789	1.034400	2.034399	0.0
2-J_2	-2848.5457576	-2848.5457576	1.033895	2.033894	0.0
2-J_3	-2848.5463811	-2848.5463811	1.033824	2.033826	0.0
2-J_4	-2848.5448069	-2848.5448069	1.033846	2.033846	0.0
2-J_5	-2848.5448575	-2848.5448576	1.033552	2.033553	0.0
2-J_6	-2848.5478575	-2848.5478599	1.034187	2.034238	1.1
2-J_7	-2848.5462659	-2848.5462659	1.033621	2.033622	0.0

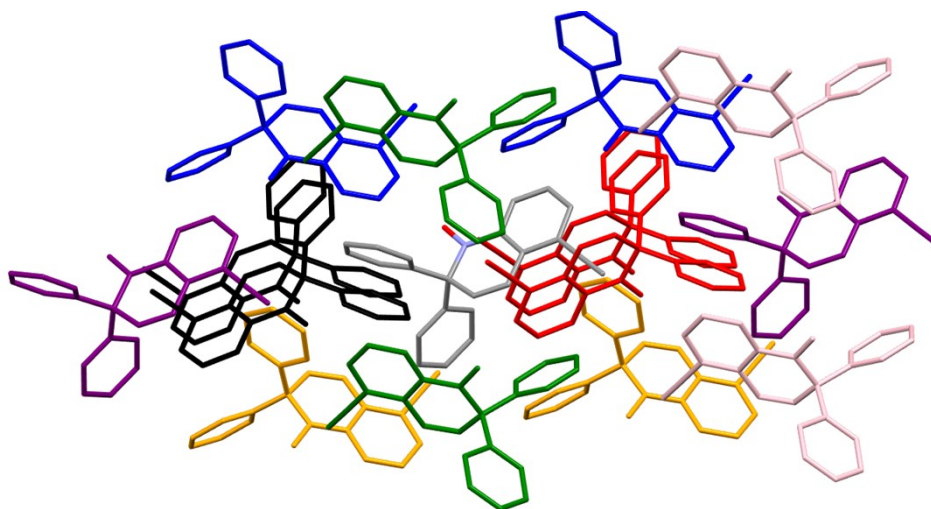


Table S7 Correspondence of name, color, and symmetry for **3**.

Contacts	Color	Symmetry
J_1	Red	$(1/2-x, 1-y, 1/2+z)$
J_2	Blue	$(-x, -1/2+y, 3/2-z)$
J_3	Green	$(1/2+x, 3/2-y, 1-z)$
J_4	Orange	$(1-x, -1/2+y, 3/2-z)$
J_5	Pink	$(1/2+x, 1/2-y, 1-z)$
J_6	Purple	$(x, -1+y, z)$
J_7	Black	$(1/2-x, 2-y, 1/2+z)$

Table S8 Calculated J value and corresponding parameters for **3**.

Compound	$E_{BS}/\text{Hartree}$	$E_T/\text{Hartree}$	$\langle S^2 \rangle_{BS}$	$\langle S^2 \rangle_T$	$2J_{\text{calcd.}}/\text{cm}^{-1}$
3-J_1	-2031.3139756	-2031.3139783	1.034065	2.034083	1.2
3-J_2	-2031.3127490	-2031.3127493	1.033829	2.033829	0.1
3-J_3	-2031.3109859	-2031.3109789	1.033639	2.033711	-3.1
3-J_4	-2031.3106214	-2031.3106215	1.033132	2.033134	0.0
3-J_5	-2031.3101704	-2031.3101703	1.033297	2.033293	0.0
3-J_6	-2031.3104721	-2031.3104721	1.033251	2.033251	0.0
3-J_7	-2031.3108973	-2031.3108973	1.033280	2.033282	0.0

^1H and ^{13}C NMR charts

1. 5-Aminoquinoline

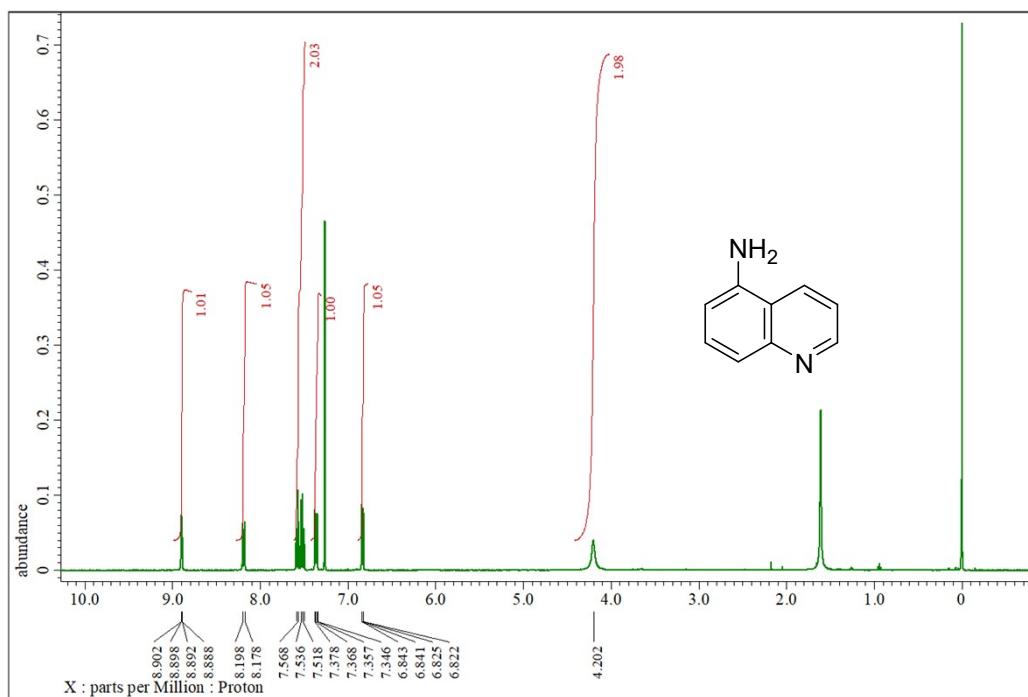


Fig. S10 ^1H -NMR spectrum for 5-aminoquinoline.

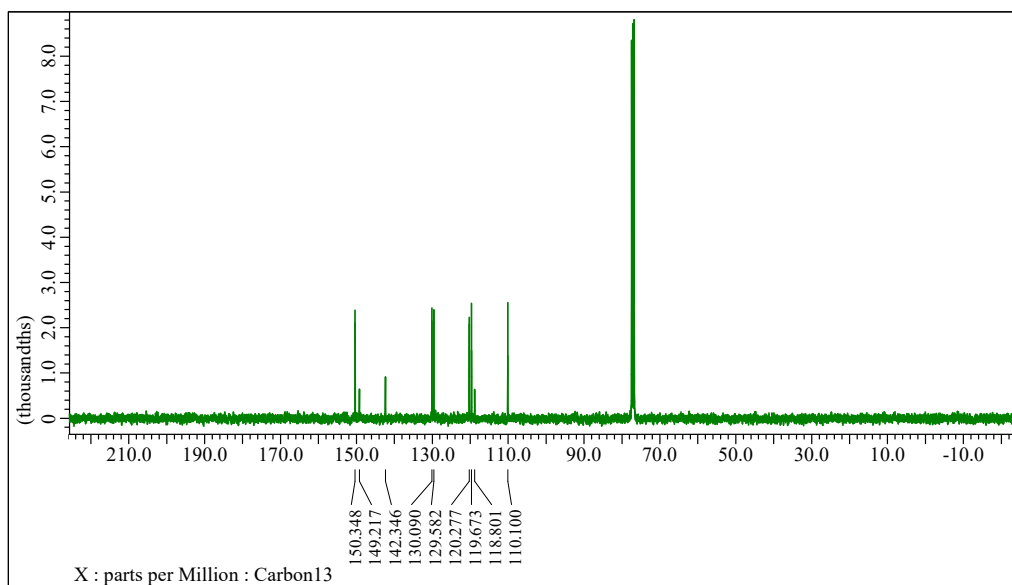


Fig. S11 ^{13}C -NMR spectrum for 5-aminoquinoline.

2. 5-Iodoquinoline

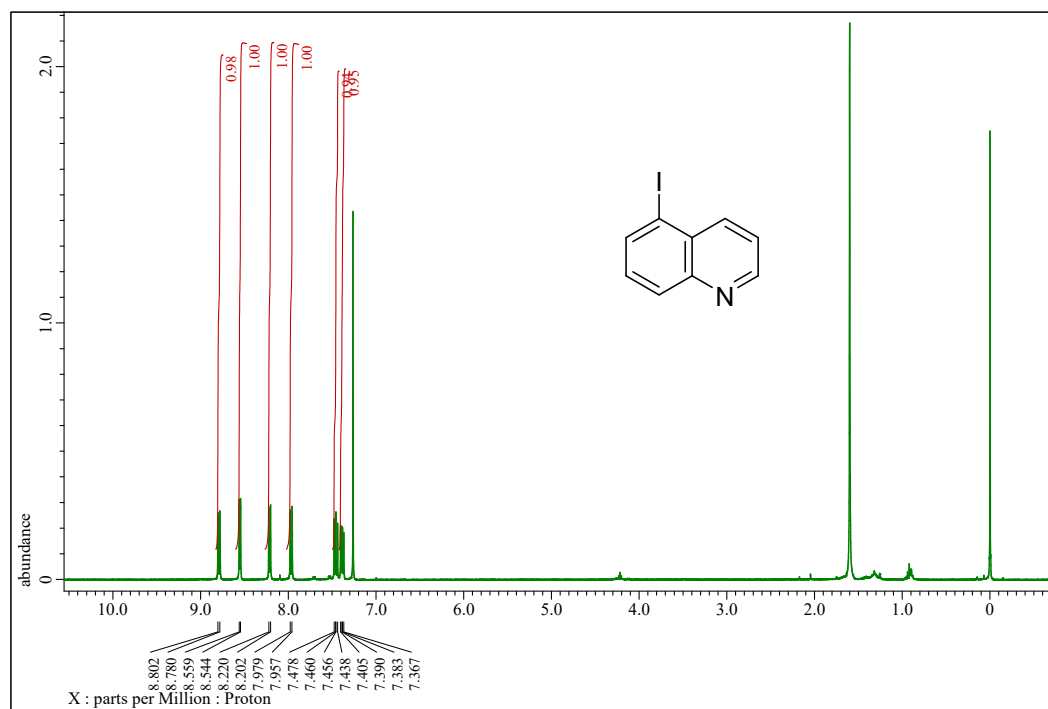


Fig. S12 ¹H-NMR spectrum for 5-iodoquinoline.

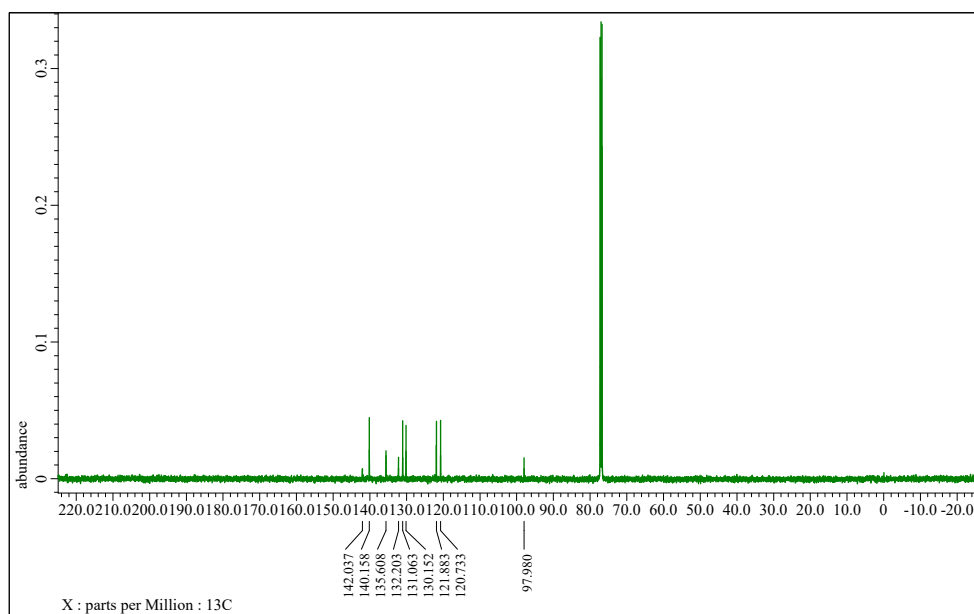


Fig. S13 ¹³C-NMR spectrum for 5-iodoquinoline.

3. 5-[2-(Trimethylsilyl)ethynyl]quinoline

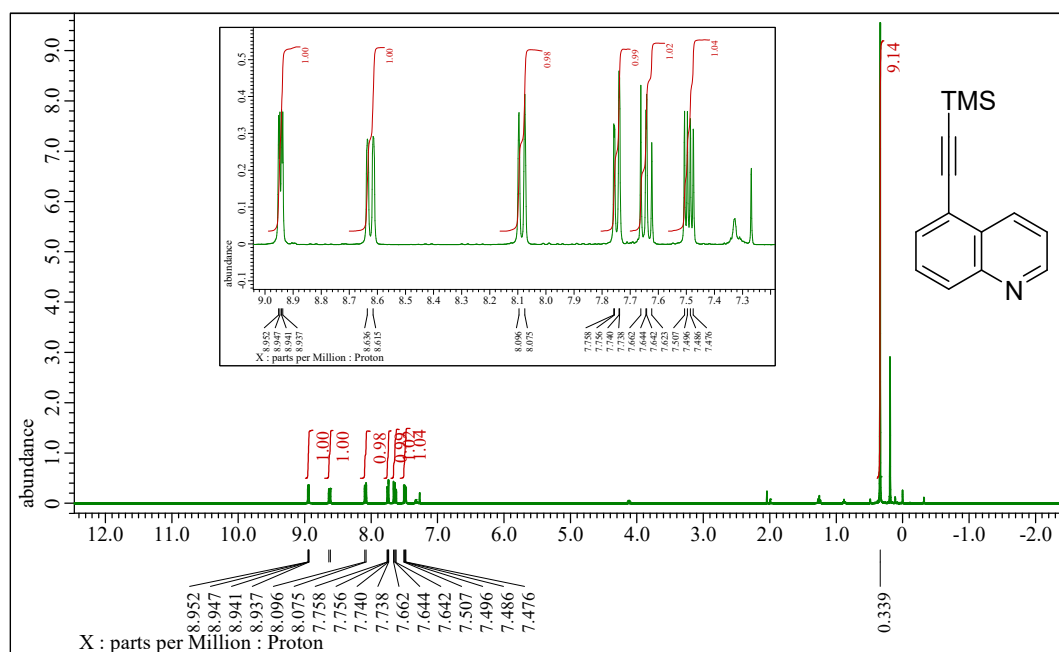


Fig. S14 ¹H-NMR spectrum for 5-[2-(trimethylsilyl)ethynyl]quinoline.

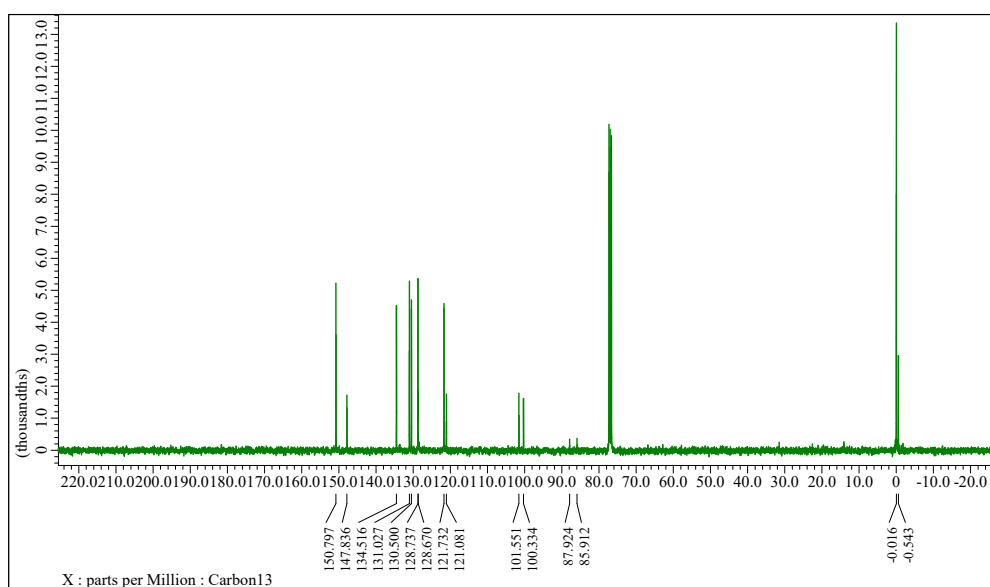


Fig. S15 ¹³C-NMR spectrum for 5-[2-(trimethylsilyl)ethynyl]quinoline.

4. 5-[2-(Trimethylsilyl)ethynyl]quinoline *N*-oxide

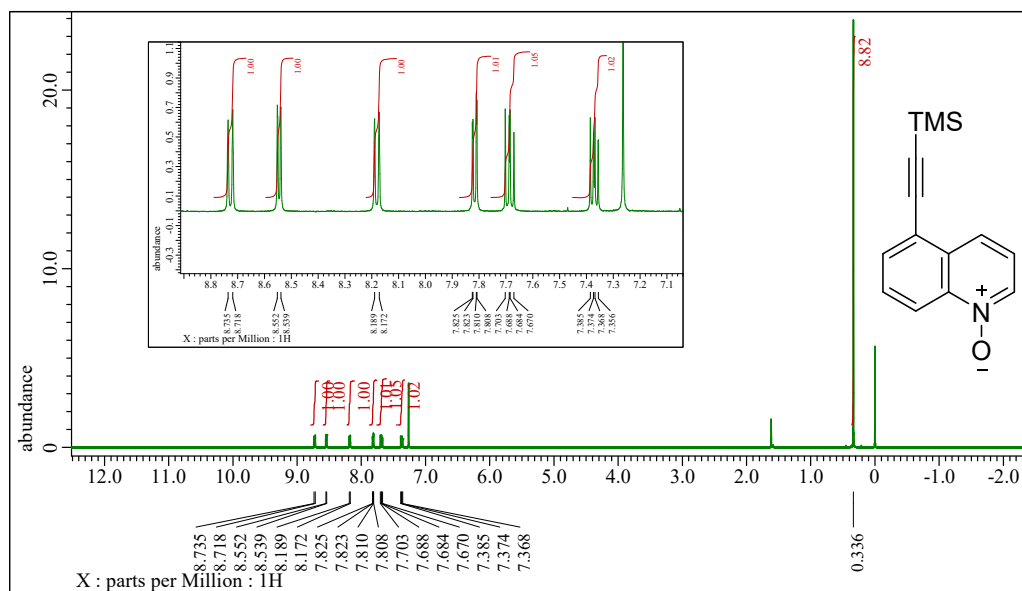


Fig. S16 ¹H-NMR spectrum for 5-[2-(trimethylsilyl)ethynyl]quinoline *N*-oxide.

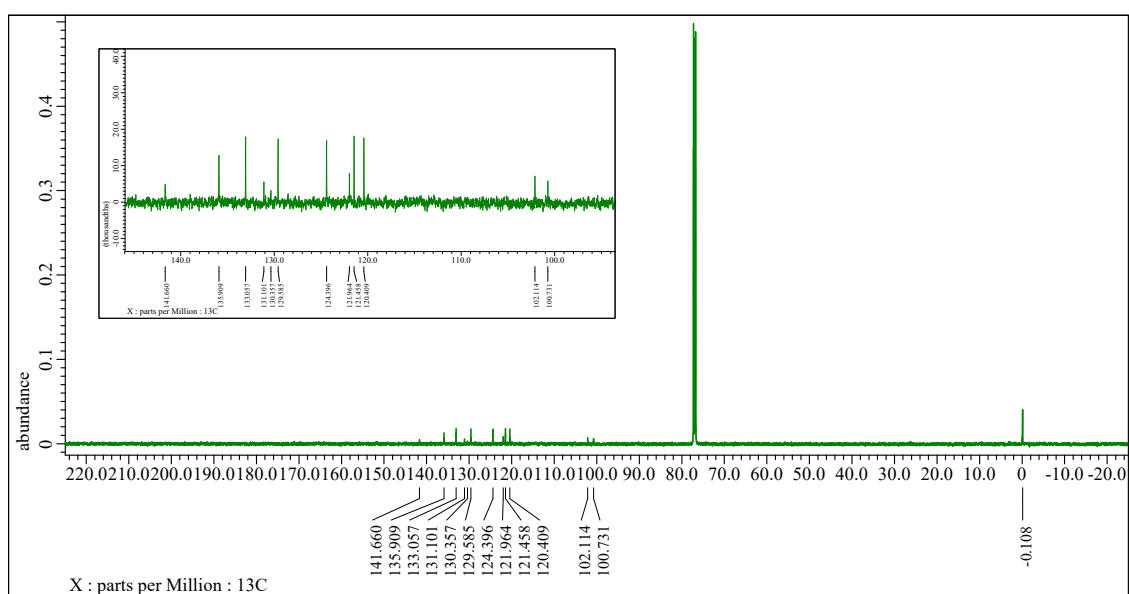


Fig. S17 ¹³C-NMR spectrum for 5-[2-(trimethylsilyl)ethynyl]quinoline *N*-oxide.

5. 5-[2-(Trimethylsilyl)ethynyl]-2-phenylquinoline *N*-oxide

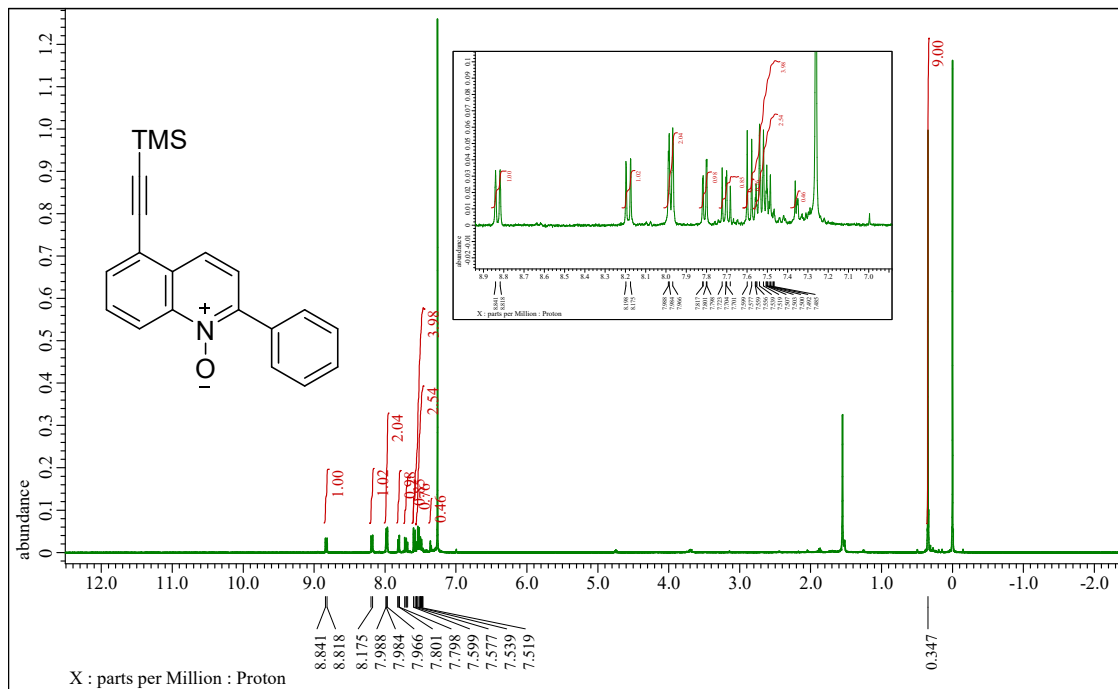


Fig. S18 ¹H-NMR spectrum for 5-[2-(trimethylsilyl)ethynyl]-2-phenylquinoline *N*-oxide.

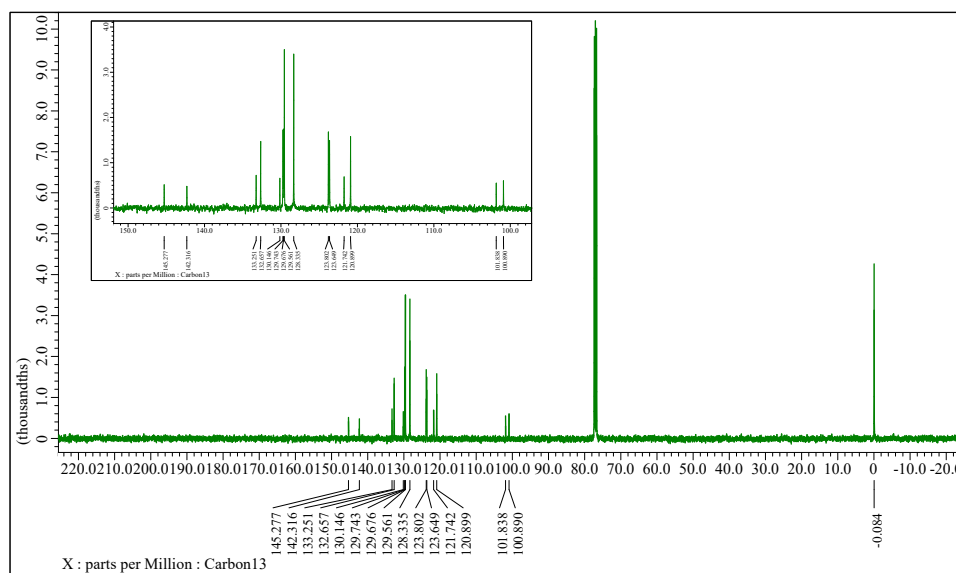


Fig. S19 ¹³C-NMR spectrum for 5-[2-(trimethylsilyl)ethynyl]-2-phenylquinoline *N*-oxide.

References

- S1. G. M. Sheldrick, *Acta Crystallogr. Sect. C Struct. Chem.*, 2015, **71**, 3–8.
- S2. Bruker AXS Inc., APEX4 v2021.10-0, Madison, WI, USA, 2021.
- S3. R. R. Gupta, in *Landolt-Börnstein: Numerical Data and Functional Relationships in Science and Technology, New Series, Group II*, eds. K.-H. Hellwege and A. M. Hellwege, Springer, Berlin, Germany, 1986, pp. 4–5.
- S4. M. J. Frisch, G. W. Trucks, H. B. Schlegel, G. E. Scuseria, M. A. Robb, J. R. Cheeseman, G. Scalmani, V. Barone, G. A. Petersson, H. Nakatsuji, X. Li, C. Caricato, A. V. Marenich, J. Bloino, J. B. Janesko, R. Gomperts, B. Mennucci, H. P. Hratchian, J. V. Ortiz, A. F. Izmaylov, J. L. Sonnenberg, D. Williams-Young, F. Ding, L. Lipparini, F. Egidi, J. Goings, B. Peng, A. Petrone, T. Henderson, D. Ranasinghe, V. G. Zakrzewski, J. Gao, N. Rega, G. Zheng, W. Liang, M. Hada, M. Ehara, K. Toyota, R. Fukuda, J. Hasegawa, M. Ishida, T. Nakajima, Y. Honda, O. Kitao, H. Nakai, T. Vreven, K. Throssell, J. A. Montgomery Jr., J. E. Peralta, F. Ogliaro, M. J. Bearpark, J. J. Heyd, E. N. Brothers, K. N. Kudin, V. N. Staroverov, T. A. Keith, R. Kobayashi, J. Normand, K. Raghavachari, A. P. Rendell, J. C. Burant, S. S. Iyengar, J. Tomasi, M. Cossi, J. M. Millam, M. Klene, C. Adamo, R. Cammi, J. W. Ochterski, R. L. Martin, K. Morokuma, O. Farkas, J. B. Foresman and D. J. Fox, Gaussian 16, Revision C.01, Gaussian, Inc., Wallingford, CT, USA, 2016.
- S5. B. Ghosh, T. Antonio, J. Zhen, P. Kharkar, M. E. A. Reith and A. K. Dutta, *J. Med. Chem.*, 2010, **53**, 1023–1037.
- S6. C. Galli, *Chem. Rev.*, 1988, **88**, 765–792.
- S7. K. Sonogashira, Y. Tohda and N. Hagihara, *Tetrahedron Lett.*, 1975, **16**, 4467–4470.
- S8. E. Ochiai, *J. Org. Chem.*, 1953, **18**, 534–551.
- S9. M. Yao, H. Inoue and N. Yoshioka, *Chem. Phys. Lett.*, 2005, **402**, 11–16.
- S10. N. S. Gulykina, T. M. Dolgina, G. N. Bondarenko and I. P. Beletskaya, *Russ. J. Org. Chem.*, 2003, **39**, 797–807.
- S11. D. R. Duling, *J. Magn. Reson. B*, 1994, **104**, 105–110.
- S12. C. Berti, M. Colonna, L. Greci and L. Marchetti, *Tetrahedron*, 1976, **32**, 2147–2151.
- S13. W. Heisenberg, *Z. Phys.*, 1928, **49**, 619–636.
- S14. O. Kahn, *Molecular Magnetism*, VCH, New York, NY, USA, 1993.
- S15. (a) G. A. Baker, G. S. Rushbrooke and H. E. Gilbert, *Phys. Rev.*, 1964, **135**, A1272. (b) J. C. Bonner and M. E. Fisher, *Phys. Rev.*, 1964, **135**, A640–A658.
- S16. . Yamaguchi, F. Jensen, A. Dorigo, K. N. Houk, *Chem. Phys. Lett.* 1988, **149**, 537.